

MIXED–MODE CRACK GROWTH AND PATH IN THREE POINT BENDING CRACKED SPECIMEN

D. A. ZACHAROPOULOS¹ & P. A. KALAITZIDIS¹ and I. C. AMAXAS
School of Engineering, Democritus University of Thrace, Xanthi 67100, Hellas

ABSTRACT

Modern engineering design has led to the recognition of the importance of fracture problems in many technological fields. Today, due to the great improvements in computer technology and computational methods, we are able to solve mixed-mode fracture problems in practical applications in an accurate and efficient manner.

The strain energy density theory can reliably predict the un/stable crack growth, in/stability of cracking and crack path in/stability in three dimensional structures with complex geometry, which are subjected to random loadings. The effects of K_I , K_{II} and K_{III} modes can also be included. In the present paper, we consider the case of a beam specimen with rectangular section in the presence of an inclined initial crack from side to side, subjected to three-point bending.

Using the finite element program Abaqus, we calculated the stresses and the displacements fields which are developed on the specimen with the necessary contour maps of strain energy density. From those fields are calculated. the stress intensity factors K_I , K_{II} and K_{III} , along the front of the initial crack With the strain energy density theory we determinate all the characteristic quantitative magnitudes and the qualitative estimations introduced by fracture mechanics.

Keywords: Crack initiation, Mixed-mode I,II and III, Crack path, SED theory, TPB specimen.

1. INTRODUCTION

The three dimensional problems in mechanics when an initial crack is present are quite complicated and usually precise analytic solutions do not exist. Although the specimen in this study has simple geometry and loading, the inclined position of the initial crack gives rise mixed-mode deformation on the crack lips. Thus, the three dimensional geometrical idealization of the specimen and the calculation of stress and displacement fields must be done numerically, usually by means of the method of finite elements. In our numerical modelling we use the FEM program Abaqus.

When the fields of the stresses is elastic at the possible site of failure, the local strain energy density is a dominant quantity, which governs the brittle fracture

and/or yielding, as has been proposed by Sih [1]. The possible site of failure can be a crack tip and basic quantity in this theory is the strain energy density factor (SEDF) S , which is defined by $S=r_o (dW/dV)$, where r_o , is the distance from crack tip and (dW/dV) is the elastic strain energy function per unit volume. The radius r_o of the core region is a scale length that separates the region of macroscopic homogeneity from those of microscopic in homogeneity and depends on the material. In three-dimensional and mixed-mode problems, the stresses intensity factors K_I , K_{II} and K_{III} , are functions of the position along the crack front. Similarly, for the strain energy density factor (SEDF), S , which is given by equation

$$S = a_{11}K_I^2 + 2a_{12}K_IK_{II} + a_{22}K_{II}^2 + a_{33}K_{III}^2 \quad (1)$$

where the coefficients a_{ij} , are calculated by expressions

$$16\pi\mu a_{11} = (3 - 4\nu - \cos\theta)(1 + \cos\theta) \quad (2a)$$

$$16\pi\mu a_{12} = 2\sin\theta(\cos\theta - 1 + 2\nu) \quad (2b)$$

$$16\pi\mu a_{22} = 4(1 - \nu)(1 - \cos\theta) + (3\cos\theta - 1)(1 + \cos\theta) \quad (2c)$$

$$16\pi\mu a_{33} = 4 \quad (2d)$$

with ν being the Poisson's ratio and μ the shear modulus of elasticity.

The basic hypotheses of the SED theory apply to any body in three dimensions Sih, [1], Gdoutos,[2], Zacharopoulos, [3], are:

- 1 *The direction of fracture initiation is toward to the point where is developed the maximum among the stationary values of the minima of the strain energy density factor S_{\min}^{\max} , if compared with other points on the spherical surface with center the failure point and radius r_o .*
- 2 *Fracture initiation occurs when the S_{\min}^{\max} , reaches the critical strain energy density factor (CSEDF) S_{cr} .*
- 3 *The length r of the initial crack extension is assumed to be proportional to S_{\min}^{\max} , such that S_{\min}^{\max}/r remains constant along the crack front.*
- 4 *For fast crack propagation, the new created surface of the crack are all the paths along which the maximum gradient of (dW/dV) prevails and is directed toward the location of developed the global maximum among the stationary values of the minima of (SEDF), which is denoted by $[(dW/dV)_{\min}^{\max}]_G$.*

The critical value S_{cr} for fracture initiation can be related direct to the ASTM, of the fracture toughness K_{Ic} , through

$$S_{cr} = \frac{(1 + \nu)(1 - 2\nu)}{2\pi E} K_{Ic}^2 \quad (3)$$

where E is the Young's modulus and ν the Poisson's ratio.

2. THE RESULTS OF APPLICATION ON THREE POINT BENDING CRACKED SPECIMEN

Computations are carried out for a cracked specimen with rectangular section as illustrated in Figure 1. The specimen has a span $2L=20$ cm, a width $h=5$ cm and a thickness $B=2$ cm. Consider the axis x coincides with the geometrical axis of the specimen and y axis is parallel with the vertical direction. An initial crack of length $a=1$ cm exists from side to side of the specimen along the z^* axis which makes an angle $\varphi=30^\circ$ or 60° , with the axis z . We assume that a force $P = 600$ N on the specimen is imposed.

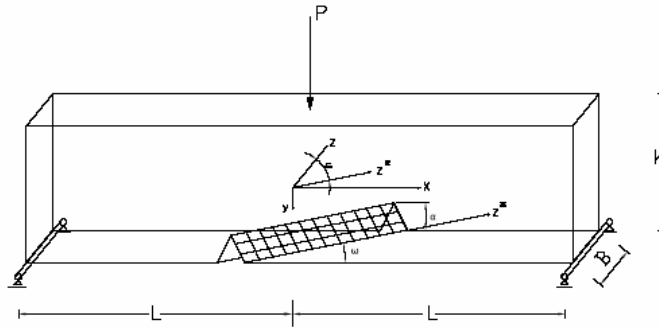


Figure 1. Geometrical characteristics of the specimen under three point bending

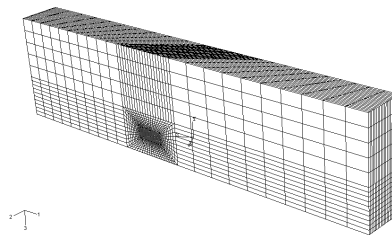


Figure 2. Finite elements mesh on the 3D-idealization of the specimen.

The material which will be used to verify the validity of the theoretical considerations is PMMA, with mechanical properties: Young's modulus $E=3000$ Gpa, Poisson ratio $\nu=0.32$, fracture toughness $K_{Ic}=1.10 \text{ MNm}^{-3/2}$, and (CSEDF), $S_{cr}=5.2563 \cdot 10^{-5} \text{ MN/m}$.

The idealized specimen is constructed with 20-nodal cubical elements around from the line of the crack tip and with 8-nodal parallelepiped elements in the remaining specimen (Fig. 2). The results from computations for manipulation of the nodal value of stresses and displacements, gave the functions of the stress intensity factors $K_I(z^*)$, $K_{II}(z^*)$ and $K_{III}(z^*)$, along the crack front, which are presented in Figures 3 and 4, for $\varphi=30^\circ$ and 60° respectively.

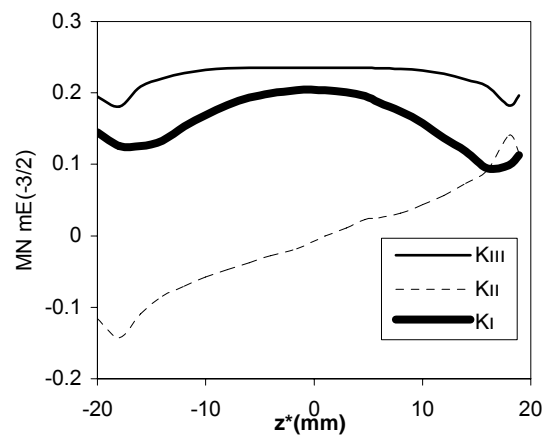


Figure 3 Variation of the stress intensity factors K_I , K_{II} and K_{III} , along the crack front for the specimen with crack angle $\varphi=30^\circ$.

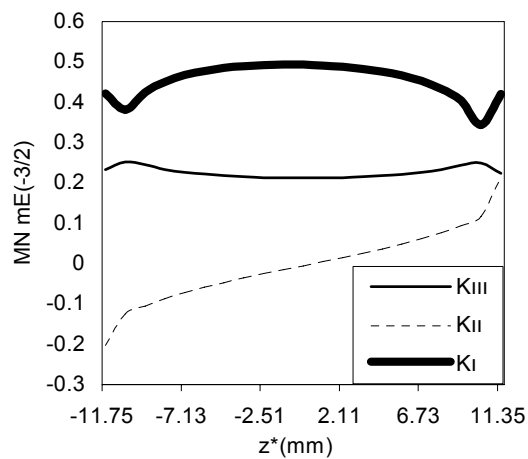


Figure 4 Variation of the stress intensity factors K_I , K_{II} and K_{III} , along the crack front for the specimen with crack angle $\varphi=60^\circ$.

Substituting the functions of the stress intensity factors $K_I(z^*)$, $K_{II}(z^*)$ and $K_{III}(z^*)$, into equations (1), the function of (SEDF), $S(z^*, \theta)$ at each point along the crack front can be obtained. According to the first hypothesis for each point of the crack tip at coordinate z^* , the angle $\theta_c(z^*)$ in the normal plane on axis z^* can be calculated. Thus, in Figures 5 and 6 we can see the variation of $S_{\min}^{\max}(z^*)$ function (SEDF), along crack front, for $\varphi=30^\circ$, and 60° respectively.

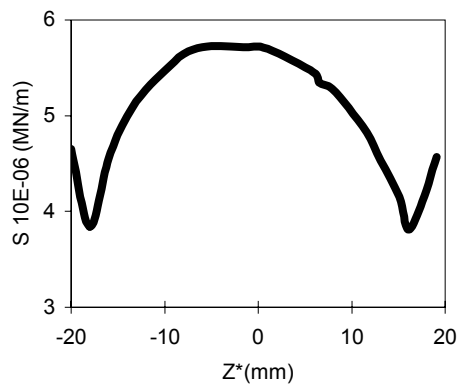


Figure 5 Variation of the strain energy density factor along the crack front for specimen with crack angle $\varphi=30^\circ$.

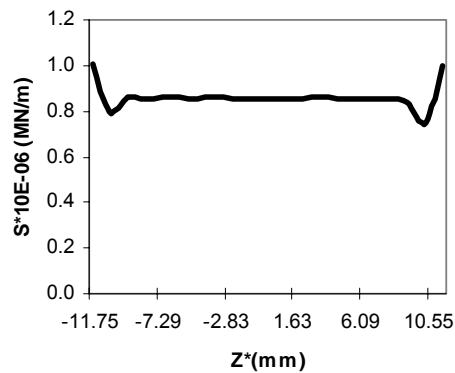


Figure 6 Variation of the strain energy density factor along the crack front for specimen with crack angle $\varphi=60^\circ$.

According to the second hypothesis the critical values of imposed force on the specimen, are: $P_{cr} = 1800 \text{ N}$ and 1300 N , for crack inclination angle $\varphi=30^\circ$ and 60° respectively. We observe that for the increase of the crack inclination angle φ , decreases the strain energy density factor. Thus increases the required imposed critical load P_{cr} . In Figures 7 and 8 the contours of strain energy density on the plane sections which coincide with the plane xy and the exterior side of the specimen respectively be shown.

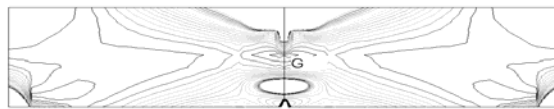


Figure 7 Map of the contours strain energy density in the plane section coincide with plane xy for the specimen with crack angle $\varphi=30^\circ$.

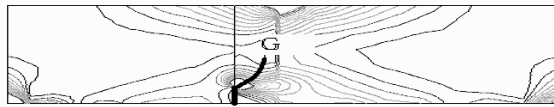


Figure 8 Map of the contours strain energy density in the exterior side of the specimen with crack angle $\varphi=30^\circ$.

Based on the hypotheses 4 and 5, we can now to draw the crack path of two points of the initial crack tip. The initial pieces of the crack path until point G, which will follow the two points of the crack tip, with solid line on the maps of the Figures 7 and 8 are drawn. The new surface of the cracking is a helicoids surface which the axis coincide with the symmetrical axis of specimen.

References

- [1] Sih G.C, Introductory chapters in Mechanics of Fracture, Vols. I to VII, ed.G.C. Sih, Martinus Nijhoff: The Netherlands (1972-1982).
- [2] Gdoutos, E. E., Problems of Mixed Mode Crack Propagation, Ed. G.C. Sih, Martinus Nijhoff: The Netherlands (1984).
- [3] Zacharopoulos, D.A., "Stability Analysis of Crack Path Using the Strain Energy Density Theory", Theoretical and Applied Fracture Mechanics, Vol. 41, pp. 327-337, 2004